https://doi.org/10.5194/hess-2022-290
Preprint. Discussion started: 2 September 2022


Hydrology and Earth System Sciences
Open Access
Discussions

# Revisiting the Hydrological Basis of the Budyko Framework With the Hydrologically Similar Groups Principle

Yuchan Chen[1], Xiuzhi Chen[1], Meimei Xue[1], Chuanxun Yang[2,3], Wei Zheng[1], Jun Cao[4], Wenting Yan[1]

[1]Guangdong Province Key Laboratory for Climate Change and Natural Disaster Studies, School of Atmospheric Sciences, Sun Yat-sen University, Zhuhai, 519082, China;
[2]Guangzhou Institute of Geochemistry, Chinese Academy of Sciences, Guangzhou, 510640, China;
[3]University of Chinese Academy of Sciences, Beijing, 100049, China;
[4]Guangdong provincial Academy of Environmental Science, Guangzhou, 510635, China;

*Correspondence to: Xiuzhi Chen (chenxzh73@mail.sysu.edu.cn)*

**Abstract.** The Budyko framework is a simple but effective tool for watershed water balance estimation. Accurate estimation of the watershed characteristic parameter (Pw) is critical to accurate water balance simulations using the Budyko framework. However, there is no universal quantification criterion for the Pw because of the complex interactions between hydrologic, climatic, and watershed characteristic factors at global scales. Therefore, this research introduced the hydrologically similar groups principle into the Budyko framework and defined the criteria for quantifying Pw in similar environments. We classified global watersheds into six groups based on watershed attributes, including climate, soil moisture, and vegetation, and identified the controlling factors of the Pw in each hydrologically similar group. Our results show that the Pw is closely related to soil moisture (SM) and the power function gradually changes from positive to negative as soil moisture increases. The relationship between the Pw and fractional vegetation cover (FVC) can be described with different linear equations in different hydrologic similarity groups, except in the group with no strong seasonality and moist soils. Based on these relationships, a model for estimating the Pw (PwM) was established with multiple non-linear regression methods between the Pw and its controlling factors (SM and FVC). Then, we used bootstrapping and runoff reconstruction methods to verify the usability of PwM. The validation results illustrate that PwM overall presents a satisfactory performance through bootstrapping ($R^2$ = 0.63) and runoff reconstruction ($R^2$ = 0.89). Results show that the hydrologically similar groups method can quantify the Pw and the improved Budyko framework can aptly simulate global runoff, especially in

https://doi.org/10.5194/hess-2022-290
Preprint. Discussion started: 2 September 2022

Hydrology and Earth System Sciences
Open Access
Discussions

humid watersheds. This study lays the basis for explaining the Pw in the Budyko framework and improves the applicability of the Budyko framework for estimating global runoff.

## 1 Introduction

There has been an increasing interest in estimating the water balance with the Budyko framework (Budyko, 1974) because it is a simple and effective tool, unlike process-based models, which typically require a large number of parameters (Caracciolo et al., 2018; Lei et al., 2014). The Budyko framework has been used for assessing linkages and feedbacks between climate forcing and land surface characteristics on water and energy cycles (Zhang et al., 2001; Milly and Shmakin, 2002; Li et al., 2013; Xu et al., 2013), prompting a great deal of empirical, theoretical, and process-based studies (Chen and Sivapalan, 2020; Roderick and Farquhar, 2011; Rau et al., 2018; Goswami and Goyal, 2022). The Budyko framework is a top-down approach relating a catchment's long-term evaporative ratio (ratio between actual evapotranspiration and precipitation) to its aridity index (ratio between potential evapotranspiration and precipitation) and is rooted on a firm physical basis (Vora and Singh, 2021; Sivapalan, 2003; Wang and Tang, 2014).

The original Budyko equation assumes that evapotranspiration is mainly controlled by precipitation (representing the availability of water) and potential evapotranspiration (representing the availability of energy) (Budyko, 1974; Wang et al., 2022). Despite its solid performance, the original Budyko equation still produces a bias between modeled and measured evapotranspiration or runoff because it does not consider the effects of watershed characteristics other than climatic conditions on water balance (Kim and Chun, 2021; Zhang et al., 2001). As a result, hydrologists have invested considerable efforts to improve model performance by introducing parameters related to watershed characteristics into the original Budyko equation. Some of the introduced parametric equations include the Fu (Fu, 1981), Zhang (Zhang et al., 2001), Choudhury-Yang (Yang et al., 2008), and Wang-Tang equations (Wang and Tang, 2014).

**Table 1.** Parametric Budyko-type formulations

| Reference | Formulation |
|---|---|
| Budyko (1974) | $\frac{ET}{P} = \left[\frac{ET_0}{P}\tanh\left(\frac{ET_0}{P}\right)^{-1}(1-exp(-\frac{ET_0}{P}))\right]^{0.5}$ |

| | |
|---|---|
| Fu (1981) | $\frac{ET}{P} = 1 + \frac{ET_0}{P} - \left[(1 + (\frac{ET_0}{P})^w\right]^{\frac{1}{w}}$ |
| Zhang et al. (2001) | $\frac{ET}{P} = \frac{1 + w\frac{ET_0}{P}}{1 + w\frac{ET_0}{P} + (\frac{ET_0}{P})^{-1}}$ |
| Yang et al. (2008) | $\frac{ET}{P} = \frac{1}{\left[1 + (\frac{P}{ET_0})^n\right]^{\frac{1}{n}}}$ |
| Wang and Tang (2014) | $\frac{ET}{P} = \frac{1 + \frac{ET_0}{P} - \sqrt{(1 + \frac{ET_0}{P})^2 - 4\varepsilon(2-\varepsilon)\frac{ET_0}{P}}}{2\varepsilon(2-\varepsilon)}$ |

These parametric equations have somewhat improved the estimation performance by taking into account the influence of watershed characteristics and thus have better estimation performance (Fu, 1981; Liu and Liang, 2015; Guan et al., 2022; Yang et al., 2008). Along with the widely used parametric equations, there has been a growing importance placed on research on the watershed characteristic parameter (Pw) as its accurate estimation is a prerequisite for the accurate simulation of evapotranspiration or runoff using the Budyko framework (Wang et al., 2022; Yao et al., 2017; Guo et al., 2019; Yu et al., 2021). Although introducing Pw improved the Budyko-type model performance, most studies failed to give a specific criterion for quantifying its value. While there is agreement that the Pw represents the integrated effects of various environmental factors (Wang et al., 2022; Liu et al., 2022; Yu et al., 2021; Gan et al., 2021), opinions differ as to what factors and effects should relate to the Pw. For instance, whether the Pw within the Budyko framework is controlled by watershed vegetation has been much debated. Some researchers advocated that vegetation plays a crucial role in the Pw, holding that there is a positive linear relationship between vegetation and the Pw (Ning et al., 2017; Zhang et al., 2018; Zhang et al., 2001). Other scholars have argued against vegetation having a strong correlation with the Pw, suggesting that most regions or some special watersheds show no significant correlation between vegetation indices and Pw (Liu et al., 2021; Li et al., 2013). Although many studies have researched the relationship between the Pw and various watershed characteristics factors, they have shown contradictory results.

https://doi.org/10.5194/hess-2022-290
Preprint. Discussion started: 2 September 2022




In fact, the relationships and interactions among hydrologic, climatic, and watershed characteristic factors are complicated by the great heterogeneity across space (Gao et al., 2018; Gan et al., 2021). Numerous studies have shown that the roles of climate and watershed characteristic factors on hydrological characteristics vary in different climatic regions (Li and Sivapalan, 2014; Trancoso et al., 2017; Singh et al., 2014). Therefore, classifying watersheds into hydrologically similar groups is essential for exploring the effect of watershed characteristics on hydrology and interpreting the physical meaning of the Pw within the Budyko framework. However, to date, relatively little research has been conducted on classifying watersheds based on the highly variable climate-Pw relationships in the Budyko framework. This may be an important reason for the contradictory research results on the Pw.

The purpose of this study was to investigate what factors and effects relate to the Pw based on the classification of hydrologically similar groups within the Budyko framework and develop a model for estimating the Pw (PwM) to simulate global runoff. We collected 726 hydrological data from globally published datasets and classified these watersheds into hydrologically homogenous regions applying the Decision Tree Regressor to measured watershed attributes. Then, we identified the controlling factors of the Pw from various environmental factors in each hydrologically similar group. Based on the relationship between the Pw and its controlling factors, the PwM was set up by multiple non-linear regression methods. This study highlights the need to account for the interactions among hydrologic, climatic, and watershed characteristic factors for explaining the Pw in the Budyko framework.

## 2 Data

### 2.1 Modeling data

Global hydrological data, including runoff (R) and corresponding precipitation (PRE), were collected from globally published datasets (726 samples listed in Supplementary Data 1, Fig. 1). Potential evapotranspiration (PET) data were downloaded from version 4.05 of the CRU TS (Climatic Research Unit gridded Time Series) climate dataset (https://doi.org/10.6084/m9.figshare.11980500), which is produced by the CRU at the University of East Anglia. For consistency, we used PET values extracted from the CRU TS dataset of all watersheds listed in Supplementary Data 1, even for studies with PET values reported.

Hydrology and Earth System Sciences
Open Access
EGU
Discussions

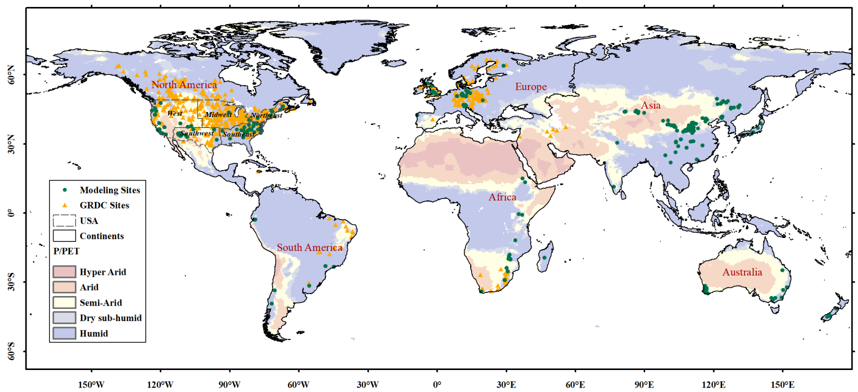


**Figure 1.** Location of the observation sites for modeling (green dots) (n = 726) and the GRDC (Global Runoff Data Centre) sites (orange triangles) (n = 545) for validation. Background colors represent P/PET.

The datasets of other watershed characteristic factors were extracted from remote sensing data. All datasets were aggregated at the same spatial resolution (0.5 degrees). The sources of datasets are summarized in Table 2.

**Table 2.** Data sources for watershed characteristic factors

| Parameter | Full name | Data source/version | Spatial/temporal resolution | Reference |
|---|---|---|---|---|
| SM | Soil moisture 15cm | GLDAS Noah Land Surface Model L4 | 0.5°/monthly | Rodell et al. (2004) |
| FVC | Fractional vegetation cover | GLASS FVC V4 | 0.5°/monthly | Liang et al. (2021) |
| SI | Seasonality Index | CRU TS dataset version 4.03 | 0.5/ multi-year average | Walsh and Lawler (1981);Feng (2019) |

**2.2 Validation data**

Observed river discharge data for validation were obtained from the Global Runoff Data Centre (GRDC, https://www.bafg.de/GRDC/EN/02_srvcs/21_tmsrs/riverdischarge_node.html). The PET and PRE values corresponding to selected sites of GRDC were extracted from remote sensing data. PET values were extracted from the CRU TS dataset. PRE values were extracted from Global Precipitation Climatology Centre (GPCC) Precipitation Total Full V2018 (0.5×0.5) data provided by the NOAA/OAR/ESRL PSL, Boulder, Colorado, USA (https://psl.noaa.gov/data/gridded/data.gpcc.html).

Hydrology and Earth System Sciences Discussions
Open Access

### 3 Methods

### 3.1 Budyko framework

This study employed the new Fu's formula (Zhou et al., 2015), a Budyko-type equation derived from Fu's equation, to analyze Pw in the Budyko framework. Within the new Fu's model, the ratio (R/P) of annual water yield (R) to precipitation (P) is determined by two variables: an aridity index (precipitation/potential evapotranspiration; P/PET), and Pw (*m*). The formula is expressed as:

$$\frac{R}{P} = \left(1 + \left(\frac{P}{PET}\right)^{-m}\right)^{\frac{1}{m}} - \left(\frac{P}{PET}\right)^{-1} \tag{1}$$

where *m* is a dimensionless integration constant varying between 1 and infinity.

Based on the randomly selected 726 samples from global hydrological studies, we derived the Pw (m) values for each sample.

### 3.2 Classification of watersheds into hydrologically similar groups using watershed attributes

A hydrologically similar group (hydrologically homogeneous region) is defined as a group of drainage basins whose hydrologic responses are similar (Kanishka and Eldho, 2020). Therefore, the relationship between Pw and a variable does not change substantially in a hydrologically similar group. However, when that relationship between Pw and the variable changes as certain boundaries are crossed, the corresponding watersheds are divided into different groups by these boundaries.

Three watershed characteristic variables — soil moisture (SM), rainfall seasonality index (SI), and fractional vegetation cover (FVC) — were selected for classification. For SM and FVC, the bounded intervals of the variables were given by the Decision Tree Regressor (DTR). The locations of splits in DTR were used as dividing intervals. The Scikit-learn library (Pedregosa et al., 2011) in Python provides the DTR used in this study. Based on Walsh and Lawler (1981), we divided the SI into three parts ($SI \leq 0.4$, $0.4 < SI \leq 0.8$, $SI > 0.8$) to represent three hydroclimatic seasonalities (precipitation spread throughout the year, marked seasonality with a short drier season, extreme seasonality with a long drier season).

Six hydrologically similar groups are detailed in Table 3.

**Table 3.** Classification of watersheds

| Soil moisture classifier | Water soil regime | Seasonality index classifier | Seasonality precipitation regime | Fractional vegetation cover classifier | vegetation cover regime | Name of the group |
|---|---|---|---|---|---|---|
| $SM \leq 20$ | Dry soil | —— | —— | —— | —— | $IN_D$ |

https://doi.org/10.5194/hess-2022-290
Preprint. Discussion started: 2 September 2022


Hydrology and Earth System Sciences
Discussions
Open Access

| | | | | | | |
|---|---|---|---|---|---|---|
| | | SI ≤ 0.4 | Seasonless | —— | —— | $IN_{WP}$ |
| SM>20 | Wet soil | 0.4 < SI ≤ 0.8 | Marked seasonality | FVC ≤ 0.2 | Low density | $IN_{WMS}$ |
| | | | | 0.2 < FVC ≤ 0.5 | Middle density | $IN_{WMM}$ |
| | | | | FVC > 0.5 | High density | $IN_{WML}$ |
| | | SI > 0.8 | Extreme seasonality | —— | | $IN_{WE}$ |

### 3.3 Setup of PwM

We performed regression analysis between the Pw and watershed characteristic variables to determine the PwM. The variables whose $R^2$ of the regression model was greater than 0.1 were selected as input variables. Then we used a polynomial as the basic model form. Each term of the polynomial depends on the regression model of the corresponding variable and the Pw. For each hydrological group, the PwM is modeled as a function as:

$$m = \sum \beta_i \times f(x_i) \tag{2}$$

where $m$ represents the value of the Pw; $x_i$ represents the input variables; $f$ corresponds to the function derived from the regression of $m$ on $x_i$; $\beta_i$ represents the empirical coefficient fitted by multiple non-linear regression (MNR).

### 3.4 Model validation

#### 3.4.1 Performance metrics

Three performance metrics were used to assess the accuracy of the PwM. The term N is the number of observations, i is the $i^{th}$ value to be simulated, and $y_s$ and $y_o$ are the simulated and observed series, respectively.

The relative bias (RelBIAS) represents systematic errors. A positive (negative) value indicates a general overestimation (underestimation), and the perfect agreement is achieved when RelBIAS is equal to zero. RelBIAS is defined as:

$$RelBIAS = \frac{mean(y_s - y_o)}{mean(y_o)} \tag{3}$$

The coefficient of determination ($R^2$) assesses how strong the linear relationship is between the simulated and the observed series. It is represented as a value between 0.0 and 1.0. The optimal value is 1 and indicates a perfect fit. It is defined as:

$$R^2 = \left\{ \frac{\sum_{i=1}^{N}(y_o^i - \bar{y}_o)(y_s^i - \bar{y}_s)}{[\sum_{i=1}^{N}(y_o^i - \bar{y}_o)^2]^{0.5}[\sum_{i=1}^{N}(y_s^i - \bar{y}_s)^2]^{0.5}} \right\} \tag{4}$$

https://doi.org/10.5194/hess-2022-290
Preprint. Discussion started: 2 September 2022




The Nash–Sutcliffe efficiency (NSE) (Nash and Sutcliffe, 1970), a goodness-of-fit index, is usually used to assess the accuracy of the model. When NSE = 1, the model predictions perfectly match the observed data. A value lower than 0 indicates that the observed mean is a better predictor than the model. It is defined as:

$$NSE = 1 - \frac{\sum_{i=1}^{N}(y_s^i - y_o^i)^2}{\sum_{i=1}^{N}(y_o^i - \bar{y}_o)^2} \tag{5}$$

**3.4.2 Bootstrapping validation**

The available data were split into training and test sets for the purpose of bootstrapping validation. A subset of 60% of the data was randomly selected without replacement for training PwM. The trained PwM was used to estimate the remaining 40% of the runoff data set, and then the performance metrics were used to evaluate the difference between the estimated and observed values. The process was repeated randomly 10000 times. We documented the model skill for each validation and showed them in a violin plot.

**3.4.3 Runoff reconstruction validation**

**(1) The runoff reconstruction by using the PwM**

To assess the accuracy of the PwM, runoff reconstructions were generated using the Budyko framework in which the value of Pw is derived from the PwM simulation.

**(2) Selection of GRDC stations and conversion of flow volumes to runoff rates**

To evaluate the estimates of runoff reconstructed by the PwM, only the GRDC stations meeting the following criteria were selected for further analysis.

1) The time series has observations within the period 2000–2016 (when corresponding SM, FVC, and SI were available).

2) The drainage area reports can be found in the original data. This criterion is designed to provide area parameters for converting original flow volumes to runoff rates.

3) The geographical coordinates reports can be found in the original data and the shape of the drainage area can be found in the GRDC Watershed Boundaries (2011). This choice was made to retrieve the geographic location of the station and then extract the corresponding required values from remote sensing data.

https://doi.org/10.5194/hess-2022-290
Preprint. Discussion started: 2 September 2022



4) Time series with unrealistic runoff rates are removed. It is generally agreed that in the Budyko framework, runoff is maximum (minimum) when m = 1 (10). Observations out of range are considered unrealistic. This criterion has been adopted to eliminate observations that are physically extremely unlikely.

Based on these criteria, 545 GRDC stations were selected for validation (Fig. 1).

Then, the flow volumes of selected sites were converted to runoff rates. The average year of catchment runoff can equal the annual streamflow measured at the outlet divided by the watershed area, provided other water losses are minimal (Ghiggi et al., 2019). Thus, runoff rates are obtained as:

$$R_{(GRDC)} = \frac{Discharge_{(GRDC)}}{Area_{(GRDC)}} \times \frac{1}{1000} \tag{6}$$

where $R_{(GRDC)}$ is the GRDC annual runoff rate (mm $yr^{-1}$); $Discharge_{\ (GRDC)}$ is the GRDC annual flow volume ($m^3\ yr^{-1}$); $Area_{\ (GRDC)}$ is the drainage area ($km^2$); 1000 is the conversion factor.

## 4 Results

### 4.1 Model for estimating Pw

Figure 2 shows the results of the regression between *m* and watershed characteristic variables for the studied watersheds within new Fu's formula and helps assess the relationship between the Pw and watershed characteristic variables.

https://doi.org/10.5194/hess-2022-290
Preprint. Discussion started: 2 September 2022

Hydrology and Earth System Sciences
Open Access
Discussions

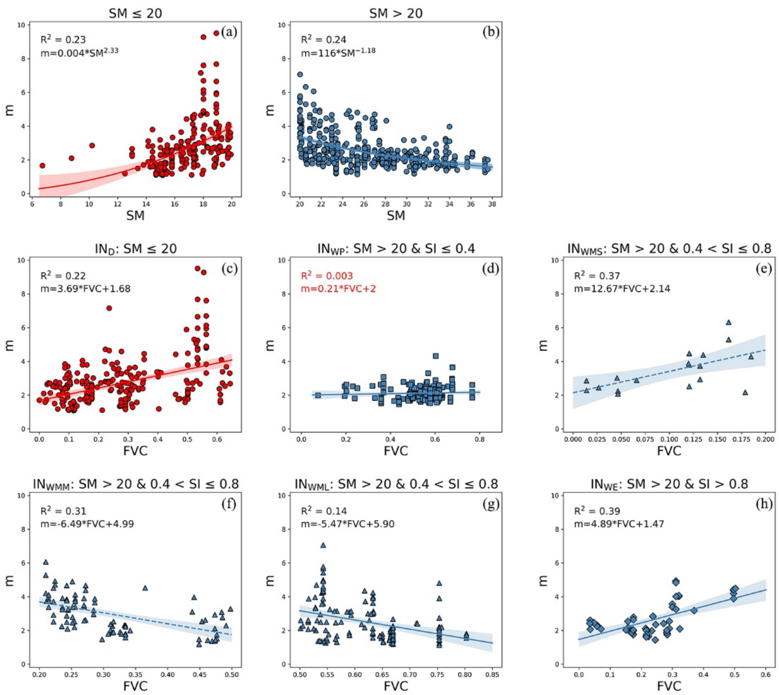


**Figure 2.** Regression between *m* with (a-b) SM (soil moisture) and (c-h) FVC (fractional vegetation cover). Symbol colors represent dry (red) and wet (blue) soil moisture. Symbol shapes indicate seasonless (square), marked seasonality (triangle), and extreme seasonality (diamond). The equation in red indicates that the input parameter is rejected in the corresponding group. The groups are defined in Table 3.

We found that the relationship between *m* and SM shows a positive power function for SM values from 0 to 20 (Fig. 2a), while there is a negative power function with SM values from 20 to 100 (Fig. 2b). The relationship between *m* and FVC shows different situations in different groups (Fig. 2c-h). The relationship between *m* and FVC can be described as a positive linear equation in the $IN_D$ group, the $IN_{WSS}$ group, and the $IN_{WE}$ group. The relationship can be described as a negative linear equation in the $IN_{WMM}$ group and the $IN_{WML}$ group. However, in the $IN_{WP}$ group, the relationship between *m* and FVC is not significant. Therefore, FVC was rejected as the input variable in the $IN_{WP}$ group.

Finally, the developed PwM is given by:

$$\boldsymbol{m} = \begin{cases} \mathbf{0.91} \times \boldsymbol{SM}^{\mathbf{0.38}} + \mathbf{1.48} \times \boldsymbol{FVC} & (IN_D, SM \leq 20) \\ \mathbf{28.72} \times \boldsymbol{SM}^{-\mathbf{0.76}} & (IN_{WP}, SM > 20, SI \leq 0.4) \\ \mathbf{39.03} \times \boldsymbol{SM}^{-\mathbf{0.96}} + \mathbf{11.82} \times \boldsymbol{FVC} & (IN_{WMS}, SM > 20, 0.4 < SI \leq 0.8, FVC \leq 0.2) \\ \mathbf{33.76} \times \boldsymbol{SM}^{-\mathbf{0.71}} - \mathbf{1.47} \times \boldsymbol{FVC} & (IN_{WMM}, SM > 20, 0.4 < SI \leq 0.8, 0.2 < FVC \leq 0.5) \\ \mathbf{20.41} \times \boldsymbol{SM}^{-\mathbf{0.42}} - \mathbf{4.221} \times \boldsymbol{FVC} & (IN_{WML}, SM > 20, 0.4 < SI \leq 0.8, FVC > 0.5) \\ \mathbf{3078} \times \boldsymbol{SM}^{-\mathbf{2.43}} + \mathbf{3.53} \times \boldsymbol{FVC} & (IN_{WE}, SM > 20, SI > 0.8) \end{cases}$$

https://doi.org/10.5194/hess-2022-290
Preprint. Discussion started: 2 September 2022



where *m* is the value of Pw; *SM* is soil moisture (kg $m^{-2}$); *FVC* is fractional vegetation cover ($m^2$ $m^{-2}$).

**4.2 Model validation**

Figure 3 helps evaluate the performance of PwM by showing the results of the global bootstrapping validation. Overall, the PwM performs well, as indicated by satisfactory skill scores (Fig. 3a). On average, the ensemble RelBIAS of the *m* simulated by the model is slightly negative, indicating a weak tendency to underestimate the values of Pw, but the maximum relative bias is less than 0.1. The interquartile range of $R^2$ for the PwM is from 0.35 to 0.40, with a median of 0.37. The scores of $R^2$ are higher than 0.3 in more than 95% of the global bootstrapping events. The global NSE skill scores show that in most bootstrapping events, the estimation error estimated variance for the PwM is less than the variance of the observations (NSE > 0), with the interquartile range from 0.33 to 0.39. Figure 3b compares the published R/P observations against those simulated by the PwM. The $R^2$ between the observed and the simulated values is higher than 0.63. The model performs well in arid and semi-arid regions. The main underestimated regions are the dry sub-humid regions and humid regions with Aridity Index values less than 1. In terms of the distribution of simulated and observed differences (Fig. 3c), the global R/P simulations are dominated by weak underestimations, of which larger underestimations occurred in western America and northwest China.

https://doi.org/10.5194/hess-2022-290
Preprint. Discussion started: 2 September 2022

Hydrology and Earth System Sciences
Discussions

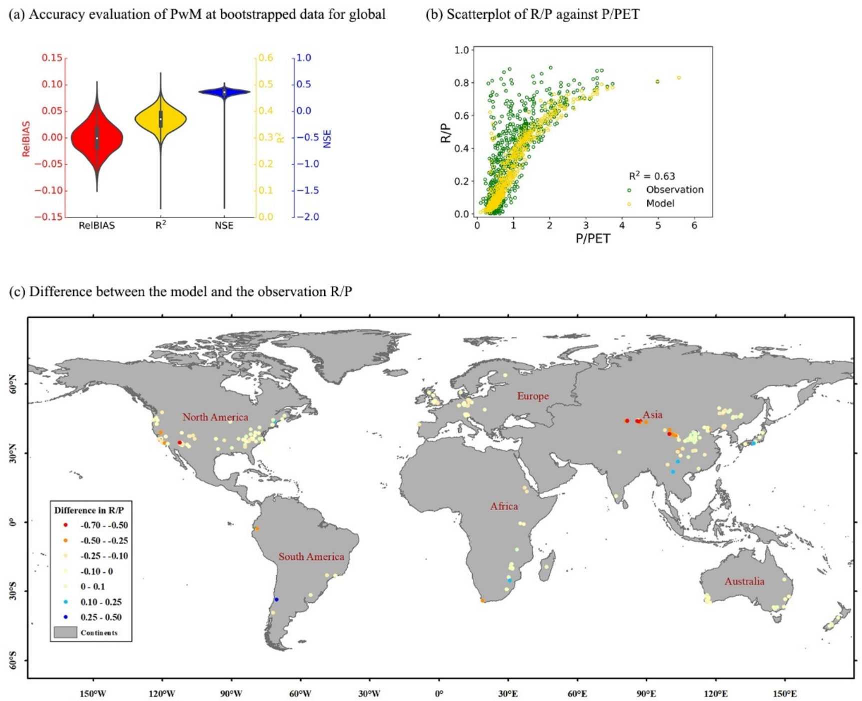


**Figure 3.** Global accuracy evaluation of the PwM. (a) Violin plot of skill scores for global bootstrapping. A violin represents the distribution of the considered skill scores of the bootstrapping validation. The white dot on the violin plot represents the median. The black bar in the center of the violin represents the interquartile range. Colors distinguish three performance metrics: Red (RelBIAS), yellow (R2) and blue (NSE). (b) Scatter plots between the R/P simulated by PwM and P/PET (yellow) and those from published data and P/PET (green). (c) Difference between the R/P values from the PmM and the published observations.

The skill scores of six intervals (Fig. 4) show more variability. Though the overall RelBIAS of the PwM is negative, the PwM tends to overestimate values of Pw in the $IN_{WP}$ group (the median of RelBIAS is positive). $R^2$ scores vary widely between groups. The $IN_{WMS}$ group scores highest in $R^2$, with a median of 0.73, and the lowest in the $IN_{WP}$ group with a median of 0.16. The grouped NSE scores show more uncertainty than the overall, especially in the $IN_{WMS}$, although the value of the lower adjacent larger than zero indicates more skill than the mean of observations, and the outliers are far below zero. The low NSE value may be due to the low number of watersheds sampled in this interval, which increased the inconclusive results.

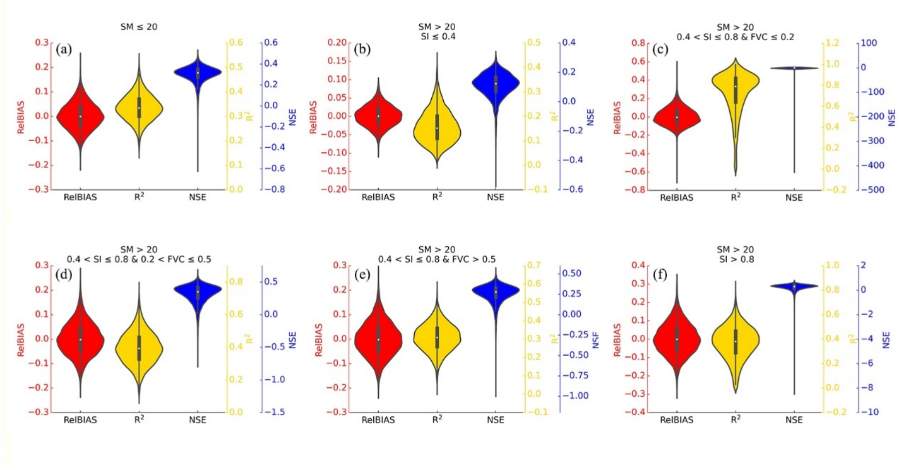


**Figure 4.** Accuracy evaluation of PwM at bootstrapped works for (a) $IN_D$, (b) $IN_{WP}$, (c) $IN_{WMS}$, (d) $IN_{WMM}$, (e) $IN_{WML}$, and (f) $IN_{WE}$.

### 4.3 Runoff reconstruction validation

The runoff reconstruction results are shown in Fig. 5. The global annual runoff estimated by the PwM ranges from 229.84 to 320.34 mm, which is slightly lower than the observed range of GRDC (265.82 ~ 345.50 mm $yr^{-1}$) (Fig. 5a). Overall, the temporal evolution of runoff is captured well in the period 2000-2010. However, since 2011, the consistency between reconstructed runoff and GRDC runoff has decreased, and the reconstruction results are constantly lower than the GRDC observations. Influenced by the underestimations in 2011-2016, the reconstructed global long-term mean runoff also shows a slight underestimation (Fig. 5b). The spatial patterns of long-term mean runoff are shown in Fig. 5c. The global estimated runoff shows lower values in the west of the United States and south of Africa, and higher values in the northeastern United States and the European Mediterranean area. Overall, the reconstructed spatial patterns are compatible with other reported findings (Ghiggi et al., 2019).

https://doi.org/10.5194/hess-2022-290
Preprint. Discussion started: 2 September 2022


Hydrology and Earth System Sciences
Discussions

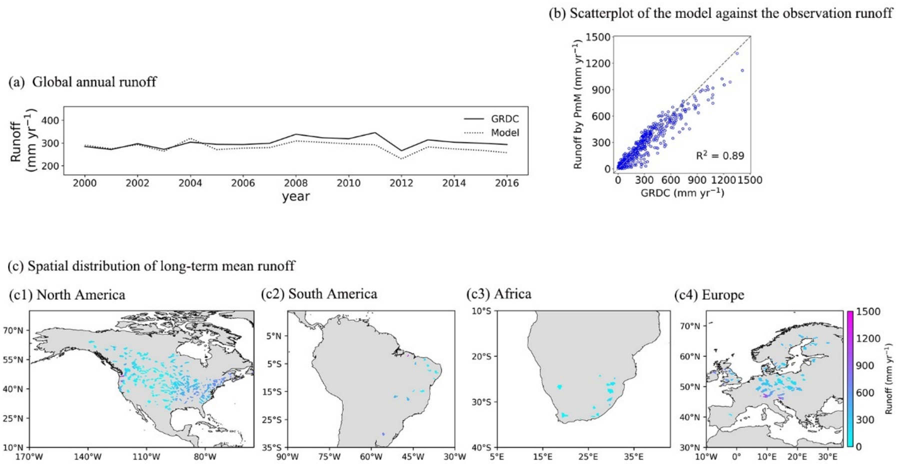


**Figure 5.** Runoff reconstruction results based on selected GRDC stations.

Figure 6 displays the considered skill scores of the reconstructed runoff obtained from each watershed of the selected GRDC ensemble from 2000-2016. It can be seen that the result of reconstruction with PwM, in general, is satisfactory, as indicated by the RelBIAS close to 0. The main area of underestimation is in the high mountains of the western United States. In the lower part of the runoff rate distribution, the runoff tends to be underestimated. Humid regions such as the northeastern United States and the European Mediterranean area have quite high $R^2$ values, while lower values are observed in semi-arid and dry sub-humid regions, which are mainly found in the western and midwestern United States. The low NSE scores tend to correspond to the watersheds where runoff is unusually under or over-estimated. Especially in the western United States, the model performance indicated by NSE decreases when runoff is underestimated.

https://doi.org/10.5194/hess-2022-290
Preprint. Discussion started: 2 September 2022

Hydrology and Earth System Sciences
Open Access
Discussions

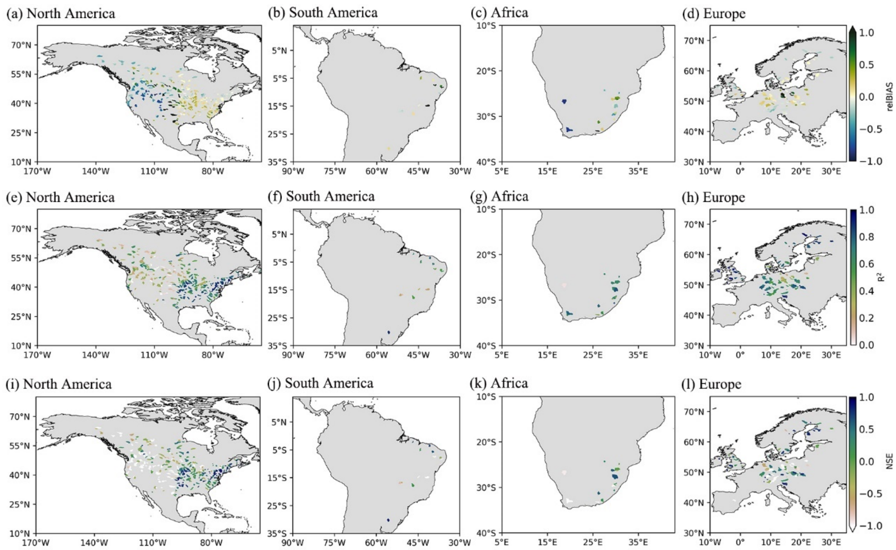


**Figure 6.** Spatial distribution of the skill scores of the reconstructed runoff.

We divided the world into nine geographic regions (Fig. 1) to further evaluate the performance of PwM on a global scale. Figure 7 shows the observational agreement of runoff time series and long-term mean for nine geographic regions. The temporal evolution of runoff is, in general, well captured, except in the western United States, where runoff was consistently underestimated. In addition, the runoff estimated by PwM is underestimated in 2011 to a greater extent than in other years. The regions where runoff was underestimated include the western United States and high latitudes in North America, and the runoff underestimation is more severe in the arid western United States than in the relatively wet northwest of North America. We considered that glacial meltwater might be the main cause of runoff underestimation. On the one hand, the spatial pattern of runoff underestimation almost coincides with that of glaciers. In glacier-covered areas, glacial snowmelt may play a more important role as a water input in arid regions than in wet ones. Therefore, the underestimation of runoff in the western United States is greater than in the northwest of North America. On the other hand, 2011 was a year in which the world generally experienced record high temperatures. The abnormal temperature might have accelerated glacier melting and altered watersheds' natural runoff yielding. The widespread underestimation in 2011 is consistent with the effect of glaciers.

https://doi.org/10.5194/hess-2022-290
Preprint. Discussion started: 2 September 2022



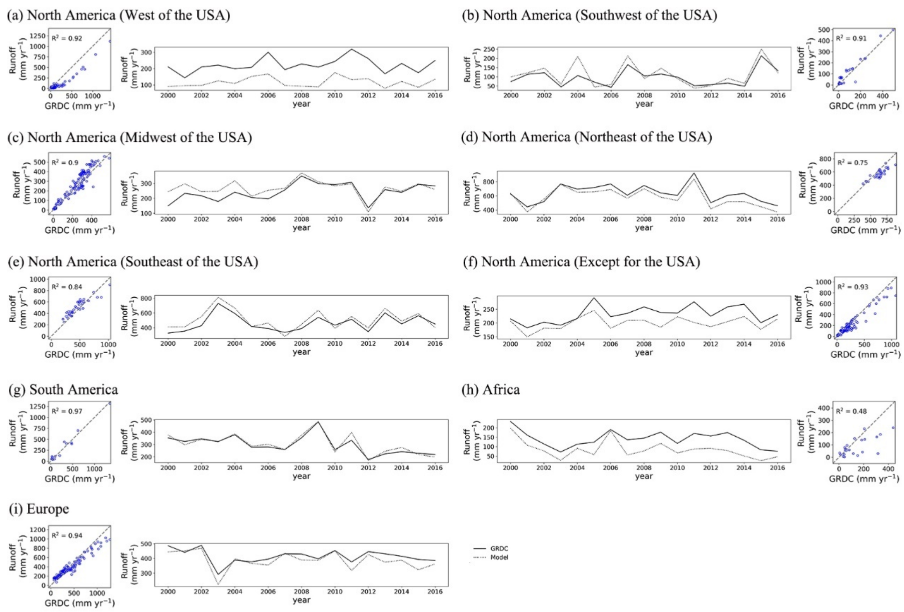


**Figure 7.** Observed versus reconstructed time series (line plots) and long-term mean (scatter plots) runoff values. The globe was divided into nine geographic regions (Fig. 1): North America ((a) west, (b) southwest, (c) midwest, (d) northeast, (e) southeast, (f) except of the USA), (g) South America, (h) Africa, and (i) Europe.

## 5 Discussion

Zhou et al. (2015) provided a Budyko equation derived from Fu's equation and confirmed that this is a valid framework for studying hydrological responses. However, the physical meaning of parameter *m*, a Pw in the Budyko equation, has remained unknown. In this paper, we selected the new Fu's equation and developed PwM, a universal framework for estimating Pw, and exploring its physical meaning. The results show that, to a large extent, PwM can estimate Pw with soil moisture and fractional vegetation. As important hydrological watershed characteristics, soil moisture and fractional vegetation cover strongly control the Pw and affect runoff by the Budyko framework.

The universal framework PwM for the derivation of Pw presented in the paper is built on empirically-based power relationships between Pw and soil moisture and linear relationships between Pw and fractional vegetation cover. Concering the power relationship between Pw and soil moisture, our findings seem to confirm those of Chen and Sivapalan (2020). However, the observed power relationship showed an evident soil moisture threshold—a positive power function appeared in the interval of 0 to 20 kg m$^{-2}$ (Fig. 2a), while a negative power function was more appropriate from 20 to 100 kg m$^{-2}$ (Fig. 2b).

The possible reason for the threshold may be that transpiration increased as the relative extractable soil water increased until reaching a soil moisture threshold value. Once the soil moisture threshold was exceeded, the acceleration of transpiration from soil moisture slowed down, and excess soil moisture provided conditions for high runoff ratios. These findings are largely in line with previous studies (Havranek and Benecke, 1978; Jiao et al., 2019; Cavanaugh et al., 2011; Ducharne et al., 1998), although the threshold of soil moisture varied in these studies (e.g., the results of Ducharne, Cavanaugh and Jiao show that the threshold value is 0.25, 0.10 and 0.20 $m^3$ $m^{-3}$, respectively).

Our study found a close linear relationship between Pw and fractional vegetation cover, and a similar linear relationship has been reported in previous studies. For example, Li et al. (2013) found that the spatial pattern of the Pw was linearly correlated with the spatial pattern of vegetation cover fraction. However, these reports were mostly from studies in large watersheds or non-humid watersheds. At the global scale, including small and wet watersheds, vegetation was considered weakly correlated with the watershed characteristic parameter of the Budyko framework (Liu et al., 2021). The classification of watersheds might provide some insights for explaining this paradox. The findings in this paper show that there were different relationships between fractional vegetation cover and Pw in different hydrological similarity groups. In dry soil watersheds ($IN_D$), the relationship between Pw and fractional vegetation cover followed a positive linear function. This finding was consistent with the majority view that vegetation transpiration increases (reflected by the increased Pw) with increasing vegetation in regions with insufficient soil moisture (Wang et al., 2012; Yao et al., 2016; Schwarzel et al., 2020). In wet soil watersheds, the relationship between vegetation and Pw also depends on the seasonality of precipitation and the size of vegetation: the relationship between the Pw and FVC could be described as a positive linear equation in the $IN_{WSS}$ and the $IN_{WE}$ groups. In contrast, a negative linear equation is needed in the $IN_{WMM}$ and $IN_{WML}$ groups. This confirms that climate, soil moisture, and vegetation are not independent factors affecting the water balance, and the physiological characteristics of vegetation greatly depend on climate and soil moisture (Gan et al., 2021; Yang et al., 2009). When vegetation was coupled with other catchment properties, the watershed characteristic parameter exhibited greater variations (Gan et al., 2021). Therefore, the classification of watersheds is crucial and supports the hypothesis that watersheds in the same class would function in a similar climate, soil moisture, and vegetation environment (Kanishka and Eldho, 2017; Sinha et al., 2019). The relationship between watershed characteristic variables and Pw may be confused without watershed classification.

https://doi.org/10.5194/hess-2022-290
Preprint. Discussion started: 2 September 2022



Although the validation showed that the overall performance of PwM was satisfactory, we noted that the accuracy of the runoff simulated by the Budyko framework in some regions was likely not optimal. Because the Pw was only forced with soil moisture, seasonality index and fractional vegetation cover, the estimated runoff could not clearly account for the effects of temperature anomalies and excess glacial meltwater on the hydrological regimes. This may be one of the reasons for the severe underestimation of runoff in western North America and southern Europe. The time series and spatial distribution results of runoff validation also point to these reasons. However, the spatial resolution of the considered remote sensing data did not allow to capture the variability of snowmelt volume governed by the unusually high temperatures. Perhaps future research could examine the relationship between watershed characteristic parameters and glacier melting caused by temperature anomalies and further improve the accuracy of runoff simulation based on the Budyko framework.

## 6 Conclusions

This research developed PwM, a universal model for estimating the Pw and exploring its physical meaning. The development of PwM using global hydrological data collected from globally published datasets and validated using GRDC observational data provides confidence in PwM. The results show that the overall performance of PwM is satisfactory. Moreover, the findings indicated that the Pw is closely related to soil moisture and fractional vegetation cover, and the relationship varies across specific hydrologic similarity groups.

Due to the complexity of hydrological processes, the PwM could not fully account for all the dynamic impacts of watershed characteristics, such as temperature anomalies and excess glacial meltwater, which might result in an underestimation of runoff in regions with glaciers. Therefore, the interactions of climate and glaciers should be explicitly incorporated into a future Budyko framework. To achieve this, detailed hydrological and glacial melt datasets at fine spatial and temporal scales are also needed.

The positive findings lay a sound basis for explaining the Pw in the Budyko framework. They could also be applied to improve global runoff estimations. We hope it will improve water balance estimates, pave the way for future hydrology research, and help consolidate water resources management studies.

*Code availability.* The pieces of code that were used for all analyses are available from the authors upon request.

*Data availability.* All data used in this study are publicly available. PET data are available from CRU TS (https://doi.org/10.6084/m9.figshare.11980500), SM data are available from GLDAS (https://disc.gsfc.nasa.gov/datasets/GLDAS_NOAH025_M_2.1/summary?keywords=GLDAS), FVC data are available from GLASS (http://www.glass.umd.edu/05D/FVC/), SI data are available from HydroShare (http://www.hydroshare.org/resource/ff287c90c9e947a78e351c8d07d9d3f3), PRE data used to model validation are available from GPCC (https://psl.noaa.gov/data/gridded/data.gpcc.html), and observed river discharge data are available from GRDC (https://www.bafg.de/GRDC/EN/02_srvcs/21_tmsrs/riverdischarge_node.html).

*Author contributions.* YC and XC designed the study and proposed the scientific hypothesis. YC implemented the experiments, conducted the analysis and wrote the paper. MX helped with data collection, and checked the technical adequacy of the experiments. CY and WZ helped with data processing. CY, WZ, CJ and WY reviewed and edited the manuscript. XC oversaw the study and conducted manuscript revision as a mentor.

*Competing interests.* The contact author has declared that neither they nor their co-authors have any competing interests.

*Financial support.* This study was financed by the National Natural Science Foundation of China (grant numbers 31971458, 41971275), Innovation Group Project of Southern Marine Science and Engineering Guangdong Laboratory (Zhuhai), grant number 311021009 and the Special High-level Plan Project of Guangdong Province (grant number 2016TQ03Z354).

**References**

Budyko, M. I.: Climate and life, Academic press1974.

Caracciolo, D., Pumo, D., and Viola, F.: Budyko's based method for annual runoff characterization across different climatic areas: an application to United States, Water Resources Management, 32, 3189-3202, 2018.

Cavanaugh, M. L., Kurc, S. A., and Scott, R. L.: Evapotranspiration partitioning in semiarid shrubland ecosystems: a two-site evaluation of soil moisture control on transpiration, Ecohydrology, 4, 671-681, 2011.

Chen, X. and Sivapalan, M.: Hydrological basis of the Budyko curve: Data-guided exploration of the mediating role of soil moisture, Water Resources Research, 56, e2020WR028221, 2020.

Ducharne, A., Laval, K., and Polcher, J.: Sensitivity of the hydrological cycle to the parametrization of soil hydrology in a GCM, Climate dynamics, 14, 307-327, 1998.

Feng, X.: Global maps of seasonality indices, HydroShare [dataset], 2019.

Fu, B.: On the calculation of the evaporation from land surface, Chinese Journal of Atmospheric Sciences, 5, 23-31, 1981.

Gan, G., Liu, Y., and Sun, G.: Understanding interactions among climate, water, and vegetation with the Budyko framework, Earth-Science Reviews, 212, 103451, 2021.

Gao, M., Chen, X., Liu, J., and Zhang, Z.: Regionalization of annual runoff characteristics and its indication of co-dependence among hydro-climate–landscape factors in Jinghe River Basin, China, Stochastic Environmental Research and Risk Assessment, 32, 1613-1630, 2018.

Ghiggi, G., Humphrey, V., Seneviratne, S. I., and Gudmundsson, L.: GRUN: an observation-based global gridded runoff dataset from 1902 to 2014, Earth System Science Data, 11, 1655-1674, 2019.

Goswami, U. P. and Goyal, M. K.: Relative Contribution of Climate Variables on Long-Term Runoff Using Budyko Framework, in: Water Resources Management and Sustainability, Springer, 147-159, 2022.

GRDC: Watershed Boundaries of GRDC Stations / Global Runoff Data Centre, Federal Institute of Hydrology (BfG) [dataset], 2011.

Guan, X., Zhang, J., Yang, Q., and Wang, G.: Quantifying the effects of climate and watershed structure changes on runoff variations in the Tao River basin by using three different methods under the Budyko framework, Theoretical and Applied Climatology, 1-14, 2022.

Guo, A., Chang, J., Wang, Y., Huang, Q., Guo, Z., and Li, Y.: Uncertainty analysis of water availability assessment through the Budyko framework, Journal of Hydrology, 576, 396-407, 2019.

Havranek, W. M. and Benecke, U.: The influence of soil moisture on water potential, transpiration and photosynthesis of conifer seedlings, Plant and Soil, 49, 91-103, 1978.

Jiao, L., Lu, N., Fang, W., Li, Z., Wang, J., and Jin, Z.: Determining the independent impact of soil water on forest transpiration: a case study of a black locust plantation in the Loess Plateau, China, Journal of Hydrology, 572, 671-681, 2019.

Kanishka, G. and Eldho, T.: Watershed classification using isomap technique and hydrometeorological attributes, Journal of Hydrologic Engineering, 22, 04017040, 2017.

Kanishka, G. and Eldho, T.: Streamflow estimation in ungauged basins using watershed classification and regionalization techniques, Journal of Earth System Science, 129, 1-18, 2020.

Kim, D. and Chun, J. A.: Revisiting a Two-Parameter Budyko Equation With the Complementary Evaporation Principle for Proper Consideration of Surface Energy Balance, Water Resources Research, 57, e2021WR030838, 2021.

Lei, H., Yang, D., and Huang, M.: Impacts of climate change and vegetation dynamics on runoff in the mountainous region of the Haihe River basin in the past five decades, Journal of Hydrology, 511, 786-799, 2014.

Li, D., Pan, M., Cong, Z., Zhang, L., and Wood, E.: Vegetation control on water and energy balance within the Budyko framework, Water Resources Research, 49, 969-976, 2013.

Li, H. Y. and Sivapalan, M.: Functional approach to exploring climatic and landscape controls on runoff generation: 2 Timing of runoff storm response, Water Resources Research, 50, 9323-9342, 2014.

Liang, S., Cheng, J., Jia, K., Jiang, B., Liu, Q., Xiao, Z., Yao, Y., Yuan, W., Zhang, X., and Zhao, X.: The global land surface satellite (GLASS) product suite, Bulletin of the American Meteorological Society, 102, E323-E337, 2021.

Liu, J., You, Y., Zhang, Q., and Gu, X.: Attribution of streamflow changes across the globe based on the Budyko framework, Science of The Total Environment, 794, 148662, 2021.

Liu, Q. and Liang, L.: Impacts of climate change on the water balance of a large nonhumid natural basin in China, Theoretical and Applied Climatology, 121, 489-497, 2015.

Liu, S., Wang, X., Zhang, L., Kong, W., Gao, H., and Xiao, C.: Effect of glaciers on the annual catchment water balance within Budyko framework, Advances in Climate Change Research, 13, 51-62, 2022.

Milly, P. and Shmakin, A.: Global modeling of land water and energy balances. Part II: Land-characteristic contributions to spatial variability, Journal of Hydrometeorology, 3, 301-310, 2002.

Nash, J. E. and Sutcliffe, J. V.: River flow forecasting through conceptual models part I—A discussion of principles, Journal of hydrology, 10, 282-290, 1970.

Ning, T., Li, Z., and Liu, W.: Vegetation dynamics and climate seasonality jointly control the interannual catchment water balance in the Loess Plateau under the Budyko framework, Hydrology and Earth System Sciences, 21, 1515-1526, 2017.

Pedregosa, F., Varoquaux, G., Gramfort, A., Michel, V., Thirion, B., Grisel, O., Blondel, M., Prettenhofer, P., Weiss, R., and Dubourg, V.: Scikit-learn: Machine learning in Python, the Journal of machine Learning research, 12, 2825-2830, 2011.

Rau, P., Bourrel, L., Labat, D., Frappart, F., Ruelland, D., Lavado, W., Dewitte, B., and Felipe, O.: Hydroclimatic change disparity of Peruvian Pacific drainage catchments, Theoretical and applied climatology, 134, 139-153, 2018.

Rodell, M., Houser, P., Jambor, U., Gottschalck, J., Mitchell, K., Meng, C.-J., Arsenault, K., Cosgrove, B., Radakovich, J., and Bosilovich, M.: The global land data assimilation system, Bulletin of the American Meteorological society, 85, 381-394, 2004.

Roderick, M. L. and Farquhar, G. D.: A simple framework for relating variations in runoff to variations in climatic conditions and catchment properties, Water Resources Research, 47, 2011.

Schwarzel, K., Zhang, L., Montanarella, L., Wang, Y., and Sun, G.: How afforestation affects the water cycle in drylands: A process-based comparative analysis, Global Change Biology, 26, 944-959, 2020.

Singh, R., Archfield, S., and Wagener, T.: Identifying dominant controls on hydrologic parameter transfer from gauged to ungauged catchments–A comparative hydrology approach, Journal of Hydrology, 517, 985-996, 2014.

Sinha, J., Jha, S., and Goyal, M. K.: Influences of watershed characteristics on long-term annual and intra-annual water balances over India, Journal of Hydrology, 577, 123970, 2019.

Sivapalan, M.: Process complexity at hillslope scale, process simplicity at watershed scale: Is there a connection?, EGS-AGU-EUG Joint Assembly, 7973,

Trancoso, R., Phinn, S., McVicar, T. R., Larsen, J. R., and McAlpine, C. A.: Regional variation in streamflow drivers across a continental climatic gradient, Ecohydrology, 10, e1816, 2017.

Vora, A. and Singh, R.: Satellite based Budyko framework reveals the human imprint on long-term surface water partitioning across India, Journal of Hydrology, 602, 126770, 2021.

Walsh, R. and Lawler, D.: Rainfall seasonality: description, spatial patterns and change through time, Weather, 36, 201-208, 1981.

Wang, D. and Tang, Y.: A one-parameter Budyko model for water balance captures emergent behavior in Darwinian hydrologic models, Geophysical Research Letters, 41, 4569-4577, 2014.

Wang, F., Xia, J., Zou, L., Zhan, C., and Liang, W.: Estimation of time-varying parameter in Budyko framework using long short-term memory network over the Loess Plateau, China, Journal of Hydrology, 607, 127571, 2022.

Wang, Y., Bredemeier, M., Bonell, M., Yu, P., Feger, K.-H., Xiong, W., and Xu, L.: Comparison between a statistical approach and paired catchment study in estimating water yield response to afforestation, Revisiting Experimental Catchment Studies in Forest Hydrology:(Proceedings of a Workshop held during the XXV IUGG General Assembly in Melbourne, June–July 2011, 3-11,

Xu, X., Liu, W., Scanlon, B. R., Zhang, L., and Pan, M.: Local and global factors controlling water-energy balances within the Budyko framework, Geophysical Research Letters, 40, 6123-6129, 2013.

Yang, D., Shao, W., Yeh, P. J. F., Yang, H., Kanae, S., and Oki, T.: Impact of vegetation coverage on regional water balance in the nonhumid regions of China, Water Resources Research, 45, 2009.

Yang, H., Yang, D., Lei, Z., and Sun, F.: New analytical derivation of the mean annual water-energy balance equation, Water resources research, 44, 2008.

Yao, J., Mao, W., Yang, Q., Xu, X., and Liu, Z.: Annual actual evapotranspiration in inland river catchments of China based on the Budyko framework, Stochastic Environmental Research and Risk Assessment, 31, 1409-1421, 2017.

Yao, W., Xiao, P., Shen, Z., Wang, J., and Jiao, P.: Analysis of the contribution of multiple factors to the recent decrease in discharge and sediment yield in the Yellow River Basin, China, Journal of Geographical Sciences, 26, 1289-1304, 2016.

Yu, K.-x., Zhang, X., Xu, B., Li, P., Zhang, X., Li, Z., and Zhao, Y.: Evaluating the impact of ecological construction measures on water balance in the Loess Plateau region of China within the Budyko framework, Journal of Hydrology, 601, 126596, 2021.

Zhang, L., Dawes, W., and Walker, G.: Response of mean annual evapotranspiration to vegetation changes at catchment scale, Water resources research, 37, 701-708, 2001.

Zhang, S., Yang, Y., McVicar, T. R., and Yang, D.: An analytical solution for the impact of vegetation changes on hydrological partitioning within the Budyko framework, Water Resources Research, 54, 519-537, 2018.

Zhou, G., Wei, X., Chen, X., Zhou, P., Liu, X., Xiao, Y., Sun, G., Scott, D. F., Zhou, S., and Han, L.: Global pattern for the effect of climate and land cover on water yield, Nature communications, 6, 1-9, 2015.